

Infrared Spectroscopy of Heavily Doped Germanium Crystals

Sergey G. Pavlov¹, Aravind N. Subramanian², R. Radhakrishnan Sumathi², S. Bin Anooz², Nikolay V. Abrosimov², Mariia Sidorova^{3,1} and Heinz-Wilhelm Hübers^{1,3}

¹ Institute of Optical Sensor System, German Aerospace Center, Berlin, Germany

² Leibniz-Institut für Kristallzüchtung, Berlin, Germany

³ Humboldt Universität zu Berlin, Germany

*corresponding author, E-mail: sergeij.pavlov@dlr.de

Abstract

Infrared absorption spectroscopy, in transmission and reflectance modes, Raman scattering spectroscopy, X-ray rocking curve imaging analytics were used to characterize optical and structural properties of *n*-type and *p*-type bulk germanium crystals doped above the Mott transition. Such materials are being considered for mid-infrared technology as a counterpart to silicon-based devices.

1. Introduction

Heavily doped (HD) semiconductors are indispensable materials for realization of electronic and optoelectronic devices in particular because their properties bridge dielectric and metallic matter [1]. However, there is a lack of a comprehensive theoretical background that adequately explains all experimentally observed optical features, especially when the latter result from spectrally overlapping strong light-matter interaction. This upsurges the importance of empirical data on these materials and its direct analysis.

Germanium (Ge) crystals offers high mobility of charge carriers and possess low lattice absorption in the mid-infrared wavelength range that makes it one of the key materials for optoelectronic applications and sensing. Most of present research on HD Ge is focused on engineering approaches for a substitutional one-electron donor doped thin (typically not above 1 μm) films deposited on various substrates. Complex techniques using epitaxial and ion implantation methods were explored to overcome the natural limits of doping [2,3]. Note that many mid-infrared applications would require a thickness of a high-quality homogeneous material that exceeds the light wavelength. Such requirements can be addressed mainly by doped bulk crystals, which therefore remain the universal platform for multi-vector semiconductor technology.

We report on the characterization of optical and structural properties of *n*-type and *p*-type Ge crystals doped with single-electron substitutional impurities above the Mott transition, up to about the equilibrium solubility limit [4-6].

2. Crystal growth and characterization

All crystals were grown by the Czochralski (Cz) method or its modified variant, the so called “mini-Cz”, with the doping from the gas phase [4]. Concentration of the free

charge carriers was estimated from calibrated resistivity measurements. The *p*-Ge crystals have large concentration of charge carriers than *n*-Ge; *p*-Ge ingots exhibit an axial doping gradient.

For the heavily doped (HD) *p*-Ge:Ga crystal (gallium concentration up to $\sim 2 \times 10^{20} \text{ cm}^{-3}$) [5] sections along this gradient (i.e. in the growth direction, Fig. 1a) were investigated. For a HD *n*-Ge:Sb (antimony concentration up to $\sim 1.6 \times 10^{18} \text{ cm}^{-3}$) and a HD *n*-Ge:P (phosphorus concentration up to $\sim 2 \times 10^{17} \text{ cm}^{-3}$), only sections perpendicular to the growth axis were measured.

The structural properties were analyzed using X-ray rocking curve imaging on the crystal sections along the growth axis. The 2D maps (intensities) of the rocking curves indicate an increased defect density at Ga concentrations above 10^{20} cm^{-3} , when HD Ge:Ga become multicrystalline.

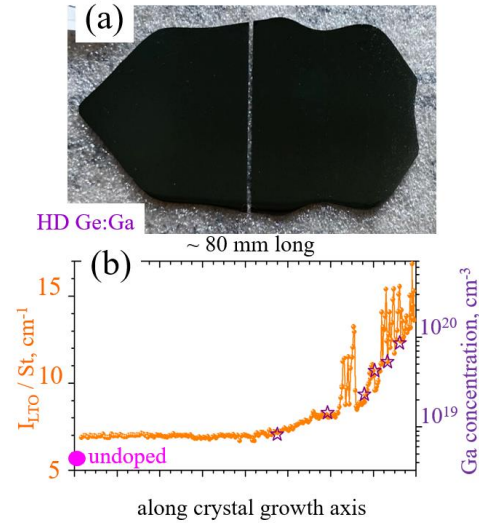


Figure 1. (a) A section along the HD Ge:Ga crystal growth (acceptor gradient) axis, the Ga concentration increases from the left to the right end; (b) Raman signal integrated absorption under the Ge LTO line over the LTO frequency, used to show the evolution of the LTO mode along the crystal growth axis; right axis – for the Ga concentration, the values marked as stars were obtained from calibrated resistivity measurements.

Raman spectra were recorded in the backscattering geometry using a WITEC 300 Alpha microscope providing a spatial resolution of 1.5 μm and a 532 nm laser. The spectra as it has been shown provide supplementary information on the concentration gradient as well as local lattice distortion (the latter – in the region of the ultra-high doping limit).

The first-order zone-centered LTO optical phonon exhibits a red shift in the energy and asymmetric line broadening. The large local deviations from the mean LTO frequency value (Fig. 1b) are most likely caused by strong structural changes, such as dislocation clusters towards the highly doped ingot end, which were observed using energy dispersive Laue spectroscopy [5].

The second-order Raman spectra show a strong increase in the scattering rates of the sum-phonon bands, expressed in line broadening, the intensity decrease of most of second-order bands and the appearance of defect-induced bands.

3. Infrared absorption spectroscopy

Infrared absorption spectra were collected with a Bruker Fourier-Transform spectrometer in transmission mode (normal incidence on the sample surface) and in reflection mode (biconic mode, $13^\circ - 13^\circ$).

Transmission spectra of HD Ge crystals do not return useful information in the mid-infrared range for crystals doped above the Mott transition. This is apparently due to the strong free carrier absorption, which affects the spectra up to the bandgap absorption for p -Ge (Fig. 2).

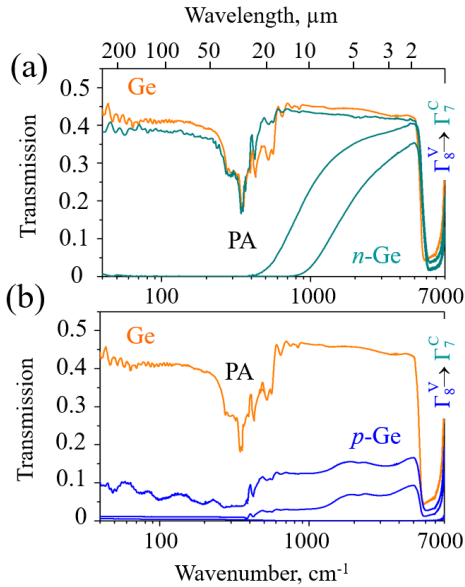


Figure 2. Transmission spectra of Ge samples doped below and above the Mott transitions, compared with the spectra of undoped Ge (residual acceptors below 10^{13} cm^{-3}). (a) Sb doped n -Ge, donor densities are $9.0 \times 10^{14} \text{ cm}^{-3}$, $5.7 \times 10^{17} \text{ cm}^{-3}$, $1.6 \times 10^{18} \text{ cm}^{-3}$; (b) Ga doped p -Ge, acceptor densities are $1.1 \times 10^{16} \text{ cm}^{-3}$, $\sim 5 \times 10^{18} \text{ cm}^{-3}$, $\sim 5 \times 10^{19} \text{ cm}^{-3}$. Interband transitions contributing to the integral absorption are shown. PA stays for multi-phonon absorption bands.

The samples doped below the Mott transitions exhibit non-vanishing transmission with the characteristic features of multi-phonon absorption (PA) bands (Fig. 2).

Infrared reflectance spectra of HD Ge reveal the impact of various optical processes contributing to infrared absorption: intraband absorption by free electrons ($e \rightarrow e$), including features associated with intervalley scattering in the conduction band of n -type Ge; intrasubband heavy and light holes ($hh \rightarrow hh$ and $lh \rightarrow lh$) and intersubband absorption by heavy-to-light hole transitions ($hh \rightarrow lh$) in p -Ge. Additionally, common for the both materials, interband absorption (dominating by) direct $\Gamma_8^{\text{VB}} \rightarrow \Gamma_7^{\text{CB}}$ transitions between the valence and conduction bands is clearly observed in the high-frequency region of the mid-infrared reflectance spectra. The frequency shift in the latter transition type illustrates the doping-induced bandgap narrowing [7] in a HD Ge.

4. Conclusions

Complementary (transmission and reflection) infrared absorption spectroscopy provides detailed information about optical properties of heavily doped germanium bulk crystals. At charge carrier densities above the Mott transition, mid-infrared transmission vanishes, while reflectance spectra indicate the transition between strong reflection and absorption regions.

Raman microscopy can be used to evaluate the local quality of HD Ge crystals, which is affected by local (dopant) and distributed (lattice) defects.

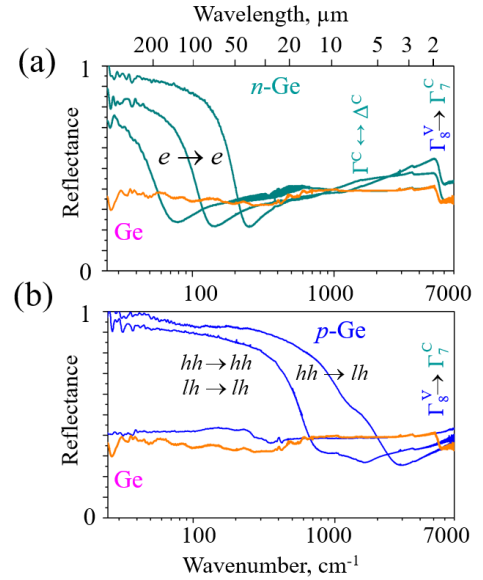


Figure 3. Reflectance spectra of HD Ge samples compared with the spectra of undoped Ge. (a) Sb doped HD n -Ge, donor densities are $1.4 \times 10^{17} \text{ cm}^{-3}$, $5.7 \times 10^{17} \text{ cm}^{-3}$, $1.6 \times 10^{18} \text{ cm}^{-3}$. (b) Ga doped HD p -Ge, acceptor densities are $1.1 \times 10^{16} \text{ cm}^{-3}$, $\sim 5 \times 10^{18} \text{ cm}^{-3}$, $\sim 5 \times 10^{19} \text{ cm}^{-3}$. Intrasubband $e \rightarrow e$, $hh \rightarrow hh$, $lh \rightarrow lh$, intersubband $hh \rightarrow lh$, interband $\Gamma_8 \rightarrow \Gamma_7$ as well as $\Gamma \rightarrow \Delta$ intervalley scattering transitions contributing to the integral absorption are shown.

Acknowledgements

The authors acknowledge partial support from the German Research Foundation (Deutsche Forschungsgemeinschaft) under DFG projects numbers 509105207 and 509113935.

References

- [1] R. A. Abram, G. J. Rees, and B. L. H. Wilson, Heavily doped semiconductors and devices, *Adv. Phys.* 27 (6): 799–892, 1978.
- [2] H. A. Tahini, A. Chronos, R. W. Grimes, U. Schwingenschlögl, H. Bracht, Point defect engineering strategies to retard phosphorous diffusion in germanium, *Phys. Chem. Chem. Phys.* 15: 367-371, 2013.
- [3] J. Kim, S. W. Bedell, D. K. Sadana, Multiple implantation and multiple annealing of phosphorus doped germanium to achieve n-type activation near the theoretical limit, *Appl. Phys. Lett.* 101: 112107, 2012.
- [4] R. Radhakrishnan Sumathi, N. Abrosimov, K.-P. Gradwohl, M. Czupalla, J. Fischer, Growth of heavily-doped Germanium single crystals for mid-Infrared Applications, *J. Cryst. Growth*. 535: 125490, 2020.
- [5] A. Subramanian, N. Abrosimov, A. Gybin, Ch. Guguschev, U. Juda, A. Fiedler, F. Bärwolf, I. Costina, A. Kwasniewski, A. Dittmar, R. Radhakrishnan Sumathi, Investigation of Doping Processes to Achieve Highly Doped Czochralski Germanium Ingots, *J. Electron. Mater.* 52: 5178–5188, 2023.
- [6] Aravind N. Subramanian, M. P. Kabukcuoglu, C. Richter, U. Juda, R. Kernke, F. Bärwolf, E. Hamann, M. Zuber, N. V. Abrosimov, R. Radhakrishnan Sumathi, Growth of Boron-Doped Germanium Single Crystals by the Czochralski Method, *Cryst. Growth Des.* 25 (4): 1075–1081, 2025.
- [7] C. Xu, J. Kouvetakis, and J. Menéndez, Doping dependence of the optical dielectric function in n-type germanium, *J. Appl. Phys.* 125: 085704, 2019.